AREAS OF SAND SEAS ON TITAN FROM CASSINI RADAR AND ISS: FENSAL AND AZTLAN. K. Arnold[1], J. Radebaugh[1], C. J. Savage[1], E.P. Turtle[2], R.D. Lorenz[2], E.R. Stofan[3], A. Le-Gall[4], and the Cassini Radar Team. [1]Brigham Young University, Department of Geological Sciences, Provo, UT 84602, *jani.radebaugh@byu.edu*.

Introduction: Thousands of linear dunes observed on the surface of Saturn's moon, Titan, were one of the greatest surprises uncovered by the Cassini spacecraft since 2004 [1,2]. As much as 15% of Titan is covered by dunes observed in Titan's equatorial regions, mainly in the form of sand seas, which are substantial in size [1,2,3]. The discovery of dunes on Titan indicates a similarity of processes between Earth, Mars, Venus and Titan [1,2] and suggests that there must be, or have been, sufficient wind, sediment supply, and collection area for the dunes to form.

Linear dunes in Cassini Synthetic Aperture Radar (SAR) images are similar in size, radar reflectivity, and morphology to linear dunes on Earth in sand seas in the Namib, Saharan, and Saudi Arabian deserts. [4]. On Titan these features likely form as tidally-driven winds sculpt drifts of organics into long linear dunes [1]. These dunes, similar to terrestrial linear dunes, interact with existing topography in diverting and reconnecting around existing topography strongly indicating the moon's prevailing wind direction, which is globally generally from west to east [5].

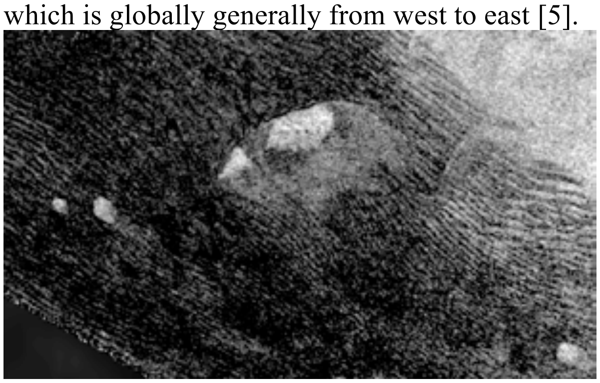

Fig 1. Linear dunes on Titan. *Note the dunes divert around topographic obstacles (Cassini Radar image, T3 region, 12° N, 35° W, about 120 x 260 km).*

To better understand the formation of dunes and sand seas on Titan we have focused our research on quantifying the areas of sand seas across Titan. Finding areas of sand seas and dune fields using Cassini SAR images has been done in a qualitative way [2] and is now being done more completely in this work and [3], but this is the first detailed study of sand sea areas using images from Cassini's Imaging Science Subsystem (ISS). Unlike SAR images, ISS images completely cover the equator, but at lower resolution [6]. Our calculations will help to further refine the organic inventory [7] and constrain hypotheses concernering the processes that govern sediment supply, transport, and deposition of grains.

Methods: For this work we studied the areas of the Fensal and Aztlan sand seas east of Xanadu. Fensal is located just north of the equator while Aztlan lies almost directly below, both centered on about 50° W longitude (Fig 2). Both sand seas are identified as darkly shaded regions in Cassini's ISS images at 938 nm [6].

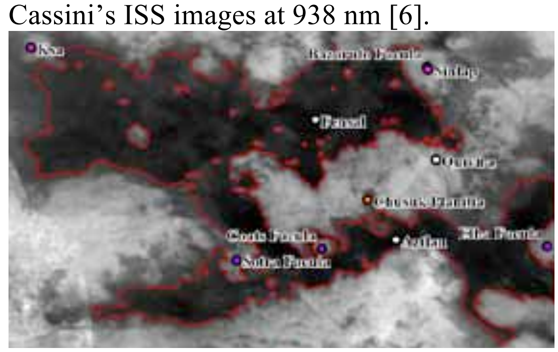

Fig 2. Fensal and Aztlan Dune Fields by Cassini's ISS. *Fensal lies to the north with Aztlan almost directly below. Red perimeter indicates estimated dune field extent based on ISS characteristics (Cassini ISS, Fensal, 5˚N 50˚W; Aztlan, 10˚S 40˚W, about 3,000 x 1,600 km).*

Calculating the areas of sand seas is challenging, given the global coverage of SAR images of ~35%. Within imaged areas, dune sands and non-dune bedrock are clearly distinguished in SAR images, so our estimates of areal coverage in imaged areas are probably good [3]. To outline dune fields and sand seas in SAR images, we choose regions containing at least 50% dune material (dark to SAR) and exclude bright mountains and other non-dune features (Fig. 3). We outlined each dune field in ESRI's ArcMap 10 on Cassini SAR image swaths, then used a geodesic calculation tool from the USGS Astrogeology division that mathematically takes into account the curvature and size of Titan to accurately represent distances and areas on the surface. From our area calculations of Fensal and Aztlan dune fields on each SAR image we can determine the percentage of SAR images covered by dunes, which is also a good beginning estimate for total percent coverage of dunes on Titan at the equatorial region.

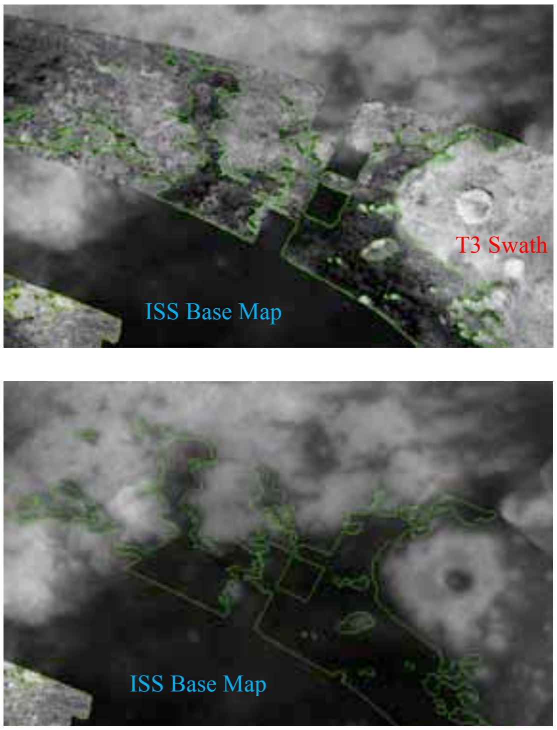

Fig 3. Dune area outlined on SAR and ISS images. *By removing the SAR swath (T3) from the top image we see that dune field areas are charaterized on the lower ISS image by darker shades. These fields were mapped on the low resolution ISS base maps to estimate total hydrocarbon grain volume on Titan (about 650 km x 1100 km).*

Given the correlation between dunes seen in SAR images and regions dark to ISS, we can map dune areas in ISS images (Fig. 4). This is done by correlating characteristics of dune areas seen in SAR images with those on our ISS base map, where resolution is much poorer but where ISS and SAR correlated. To increase the accuracy in determining which areas are darkest, we adjusted the table from monochrome to a range from yellow to purple with yellow indicating the smallest values and the areas most likely to represent sand dunes (Fig. 4). This yields a fairly good correlation between dunes seen in SAR images and those in ISS images (Fig. 4), increasing our confidence in this method. Dune areas are slightly overestimated near Sinlap and in portions of the land region between the sand seas.

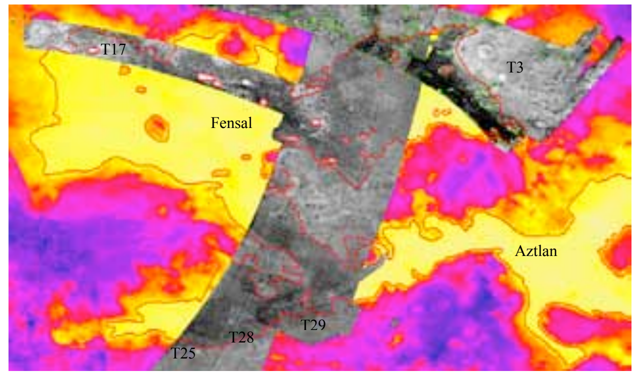

Fig 4. Fensal and Aztlan dune areas outlined on SAR/ISS images. *Note that dunes mapped on SAR image swaths correlate well to ISS estimations with only slight deviations (Cassini ISS, Fensal, 5˚N 35˚W; Aztlan, 10˚S 30˚W, about 3,000 x 1,600 km).*

Results: We have found the total area of dunes in Fensal/Aztlan in the SAR swaths to be 6.6×10^5 km^2 and in the ISS images to be 2×10^6 km^2. The ISS dune area is similar to the combined area of the Libyan and Egyptian sand seas. Future work includes measurements of areas of other sand seas and dune fields across Titan, including Belet, Shangri-La, and Senkyo. These measurements will help us determine the volume of hydrocarbon sands on Titan.

These data will help us better understand the dune forming processes that have occurred and may still be occurring on Titan.

References: [1] Lorenz R. D. et al. (2006) *Science* 312, 724-727. [2] Radebaugh J. et al. (2008) *Icarus* 194, 690-703. [3] LeGall et al. *Icarus* in review. [4] Radebaugh J. (2010) *Geomorphology* 121, 122-132. [5] Tokano T. (2010) *Aeolia* 4, 003. [6] Turtle et al. (2009) *GRL* 37. [7] Lorenz, R.D. et al. (2008) *GRL* 35.